NIPES

Journal of Science and Technology Research

Journal homepage: www.nipesjournals.org.ng

Taguchi and RSM in the Development of Cip-Parrafin-Oil Based Magneto-Rheological Fluid Enhanced with Grease

Eyere Emagbetere[a*]; Anthony O. Egorerhua[b]; Joseph O. Oyekale[c]; Chrostopher I. Ajuwa[d]

[a,b,c,d]Department of Mechanical Engineering, Federal University of Petroleum Resources, Effurun, Nigeria
emagbetere.eyere@fupre.edu.ng

Article Info

***Keywords*:**

MRF additives, smart materials, mineral oil application, magnetic materials, magnetic particles

Received 06 April 2022
Revised 14 May 2022
Accepted 18 May 2022
Available online 10 June 2022

https://doi.org/10.37933/nipes.e/4.2.2022.6

https://nipesjournals.org.ng

Abstract

Magneto-Rheological Fluids (MRF) are smart materials whose rheological properties can be suitably controlled. They are finding wide applications today in several engineering fields. However, the high cost of silicone-based MRF which is well researched and commercially available impacts negatively on the applicability, thereby necessitating improvement via further research. This work aims to develop and characterize a novel MRF that is suitable for flow-mode applications from cheap and readily available constituting materials. Carbonyl-iron particles (CIP) of size ranging 3µm to 5µm, low viscosity paraffin oil and Lithium grease were used as magnetic particle, carrier fluid and additive, respectively. Based on different mixing proportions that were determined with both Response Surface Methodology (RSM) and Taguchi method, a total of thirty one (31) samples were prepared following standard procedure. For each and all of the samples, the values of viscosity were determined using a rheometer with incorporated magnetic device, the yield stress was determined using Bingham model, and the sedimentation ratio was measured by observation method. Results showed that viscosity as well as the yield stress increases with added amount of Carbonyl-iron particles (CIP), while sedimentation ratio was inversely proportional to the percentage of added additive and carbonyl-iron particles (CIP). Carbonyl-iron particles (CIP) had the most influencing effect, and 60% CIP and 3% additives were found to be the optimum proportion. Conclusively, a new type of MRF was developed, characterised and shown to offer satisfactory responses suitable for flow-mode applications.

1. Introduction

Magnetic particles such as carbonyl iron and ferrite are widely applied to develop magneto-rheological materials. They are smart materials that change their rheological behaviour when a magnetic field is induced. Many different types of magneto-rheological materials have been developed over the years [1]–[3]. Some common types are magneto-rheological foams, magneto-rheological elastomers, magneto-rheological gel, magneto-rheological grease, ferro fluid, and magneto-rheological fluid [4]. Magneto-rheological fluid was the first to be developed among them

all and is characterized by certain favourable qualities such as ease of preparation, quick response and insensitiveness to impurities [5]. They, thus, stand out as the magneto-rheological materials with tremendous potential for engineering applications.

Magneto-rheological fluid (MRF) is of different classes based on its composition and properties. They are developed by dispersing micro-scale magnetic particles in a carrier fluid and adding some additives to enhance their properties [6]. Some popular magnetic particles used to develop MRF are carbonyl iron, ferrite, cobalt and Nickel alloys, of which the carbonyl particle is the most applied due to its high magnetic saturation and permeability [7]. The base fluid can be any fluid that is a polar liquid such as water, a non-polar solvent such as mineral oil or synthetic material. The selected fluid is usually based on its suitability for the desired application [8]. To address the problems that are associated with MRFs [3]: sedimentation, agglomeration, corrosion and shear thickening, specific additives are usually added. Different addictives used for different purposes are listed in the review by [9]. There are limitless research opportunities in developing novel MRF that can favourably compete with the carbonyl-silicone MRF in cost and effectiveness. But the main challenges with MRF, in general, are sedimentation, dispersibility and agglomeration [10]. Moreover, Wang et. al, [11] informed that the use of MRF in many devices has greatly been impeded by settling stability, cost implication and their durability. Quite a lot has been reported on additives to address sedimentation issues [9], [12]–[14]. However, the formulation of low-cost MRF remains a concern. Discovering low-cost base fluid with acceptable properties can help address this problem and increase MRF application in several fields. Preliminary studies have suggested that mineral oil (castor oil) has excellent prospects [15]. Consequently, there is a need to research further into the potential uses of mineral oil, which is cheap and quite available in MRF formulation.

This study aims to develop an MRF from locally available paraffin oil enhanced with grease that is suitable for applications in flow-mode devices. Therefore, the following objectives were pursued: Sourcing and procurement of suitable materials, design of experiments using RSM and Taguchi experimental design, conduction of experiments, analyzing the experimental results, and optimization with DOE tools. Paraffin oil may not be more suitable than silicone oil for MRFs but its relatively cheap cost and availability can be a competitive factor for its application in the formulation of MRFs. More so, this research work would guide the broad characteristics of carbonyl paraffin oil-based MRF on the usefulness of its application in flow-mode mechanical devices. Moreover, there is also a strong possibility of adopting the MRF in other areas where cost is of utmost concern.

2.1 Materials

The carbonyl iron particles (3-5μm), were obtained from Chengdu Huarui Industrial Co. Ltd, China. The particle diameter ranged from 3μm to 5μm. Paraffin oil was obtained from O and J Chemical Store, Delta State. The properties of the paraffin oil are: viscosity of 32 mPa, density of 0.8 g/cm3 at room temperature. Lithium Grease was purchased at Auto spare part market along Wari/Sapele road Effurun Delta State to serve as the additives for this study. Its properties are: Density 997 kg/m3, Viscosity 0.89 mPas Boiling point is 100^{C}.

2.2 Equipment

The equipment used for this project includes measuring cylinders, beakers, conical flask, rubber bowl, spatula, mixer, electromagnet, gaussmeter, filter paper, funnel, beam balance, mechanical stirrer, rheometer, and viscometer.

2.3 Experimental design

Three input variables were considered. They include CIP (wt%), grease (wt%) and base fluid (wt%). All input variables are taken as three levels, while the weight of the base fluid was kept constant. The Taguchi and RSM were carried out using Minitab (version 18). The optimum condition for best performance was determined using Box- Behnken Design (BBD) under RSM. The interaction effects of the variables and the response were studied using Taguchi with a rotatable option. The limits used for all factors for RSM and Taguchi are listed in Table 1.

Table 1: Factors and range for the Experimental Design

Factors	Name	Low Level	High Level
A	Volume of Paraffin	99.90	100.10
B	Weight of CIP (wt%)	40.00	70.00
C	Weight of Additives (wt%)	1.00	3.00

2.4 Error analysis

The effectiveness of the techniques was assessed using R-square values for both Taguchi and RSM. The error values were calculated based on Equation 1.

$$R^2 = 1 - \frac{\sum(y_i - \hat{y}_i)^2}{\sum(y_i - \bar{y})^2} \quad (1)$$

Where y_i is ith experimental term, $\hat{y}_i$ is the ith predicted term, $\bar{y}$ is the average of the experimental values.

2.5 Method of preparation

During the preparation of MRFs, the quantity of carbonyl particles was varied between 35-70 wt.%, by weighing on an electronic balance to ascertain its actual weight. The addictive was varied from 1-3% by weight of paraffin oil. An experimental design was done using Taguchi and Roughness Surface Methodology (Box-Behnken design). The percentage of CIP and additive by weight were taken as the two factors, while sedimentation rate and viscosity were measured as the responses.

The mixed constituents was stirred using a mechanical stirrer for 10 minutes for each sample. Firstly, the CIP was mixed with the grease and stirred for 10 minutes, and then the mixture was poured into a beaker of measured paraffin oil and stirred for another 10 minutes.

2.6 Measurement of magneto-rheological properties

MRFs' rheological properties such as shear stress and shear strain were determined using a rotational rheometer (a plate and a plate type). 0.5mL of MR fluid was infused into the 0.5mm gap between both plates of the rotational rheometer. The experiments were performed in a shear rate mode within the shear rate range from 0.01 to 250 s^{-1}. The electric current was continuously generated using a power generator of 200-220 volts. Freshly prepared samples were used in obtaining all rheological

data, and each data was collected 3 times to guarantee precision and reliability of the obtained result. Rheological data for each property were compiled, and the average was calculated. The experiment was repeated for varied magnetic fields. And then the Bingham model was used to estimate the yield stress for each case.

The rheological properties of the stabilizer samples in the oil were measured using a strain-control type cone and plate rheometers. Steady flow characteristics were measured for shear rate ranging from 0.01–1000 s^{-1}.

Several experiments were carried out to study the effects of various additives on MRF behaviour. They were performed to establish the role of the additive in the linear viscoelasticity regions. The MRF test samples were subjected to the same initial conditioning before each test run. The magnetic field was also applied before each test to develop the fluid's field-induced structures.

2.7 Determination of sedimentation stability

Stability tests must be carried out on MRFs to ensure the proper and required rheological response. The visual inspection or direct method was applied to determine the developed MRFs' stability. Each MRF was poured into a 10 mL graduated cylinder and left at rest. After one day (24 hrs), the height of an oil layer formed in the upper of the cylinder was measured to calculate the sedimentation ratio defined in Equation 2.

$$R_{sed} = \frac{H_{sp}}{H_{sp}+H_{st}} \qquad (2)$$

The height of the suspended phase (H_{sd}) and the settled phase (H_{st}) were obtained using a calibrated beaker containing the MRF sample, R_{sed} is Sedimentation ratio, H_{sp} is the height of suspended particles or phase, H_{st} is height of settled particles or phase.

3.0 Results and Discussion

3.1 Taguchi analysis: Effect of influencing factors on the responses

The effects of the factors on the means of the responses are ranked in

Table 2. It was observed that the additives have the highest effects on the means having Delta values of 6.41, thus ranked as first before the CIP, which had Delta value of 6.25. The implication of this is that the mean values of additive would be affected more by varying the factors for the Taguchi design.

Level	% ADD	% CIP
1	20.81	13.75
2	17.96	16.99
3	16.7	19.13
4	14.4	20
Delta	6.41	6.25
Rank	1	2

Level	% ADD	% CIP
1	20.81	13.75
2	17.96	16.99
3	16.7	19.13
4	14.4	20
Delta	6.41	6.25

Table 2: Response Table for Rank 1 2 **Means**

The effect of additives on the standard deviations is higher than that of the CIP, as observed in Table 3. The effect is higher on the additive, indicating that higher deviations would be observed with additives than with CIP as the factors were varied.

Table 3: Responses Table for Standard Deviations

Level	% ADD	% CIP
1	26.72	17.43
2	23	21.83
3	21.35	24.74
4	18.35	25.42
Delta	8.37	7.99
Rank	1	2

Figure 1 shows the main effects of the variables on the responses. CIP has the more significant effects on the Means, as the slope between points in the means is observably higher than the slopes between corresponding points of the additives on the plot. On average, experimental runs with CIP had much higher Means than experimental runs with the additives.

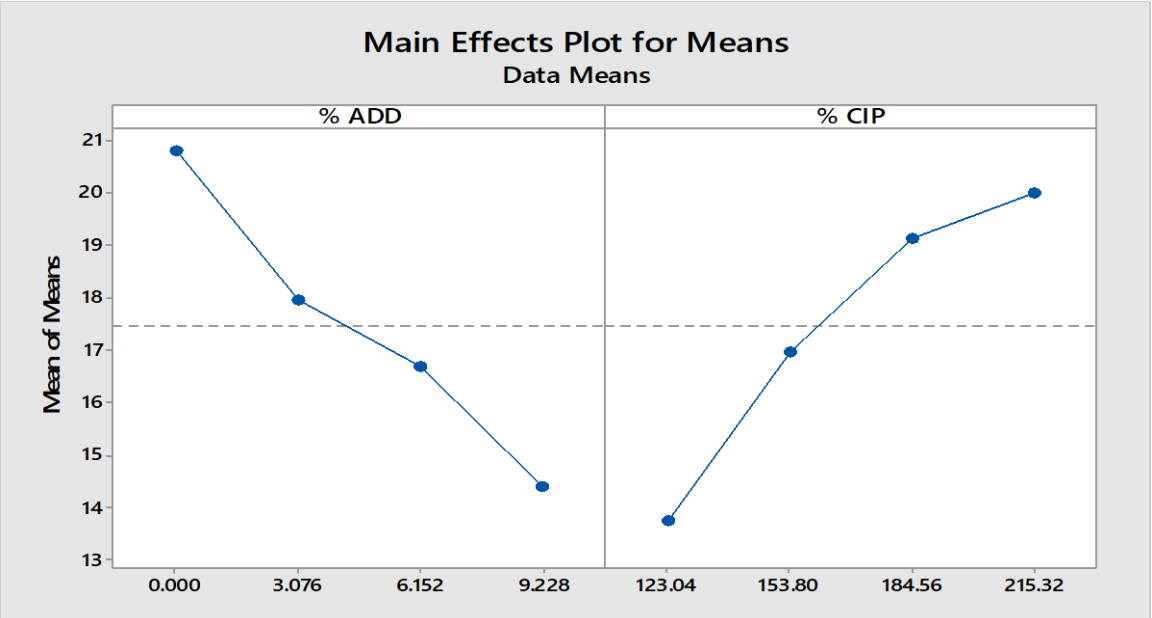

Figure 1: Main effects Plot for means

The interactions between the different input variables obtained by plotting the average of the two variables at each level are shown in Figure 2 for the interactions plot of means, and the graphs are close to parallel. As can be observed, the 3rd and 4th levels of the factors has the least interactions, as they formed the best parallel paths in the curves shown. In contrast, the first two factors showed the least interactions, showing a level of convergence and divergence in the Additive and CIP parts, respectively. The first level of the additive has a higher value of means, whereas the fourth level of CIP has a higher means value in the curve.

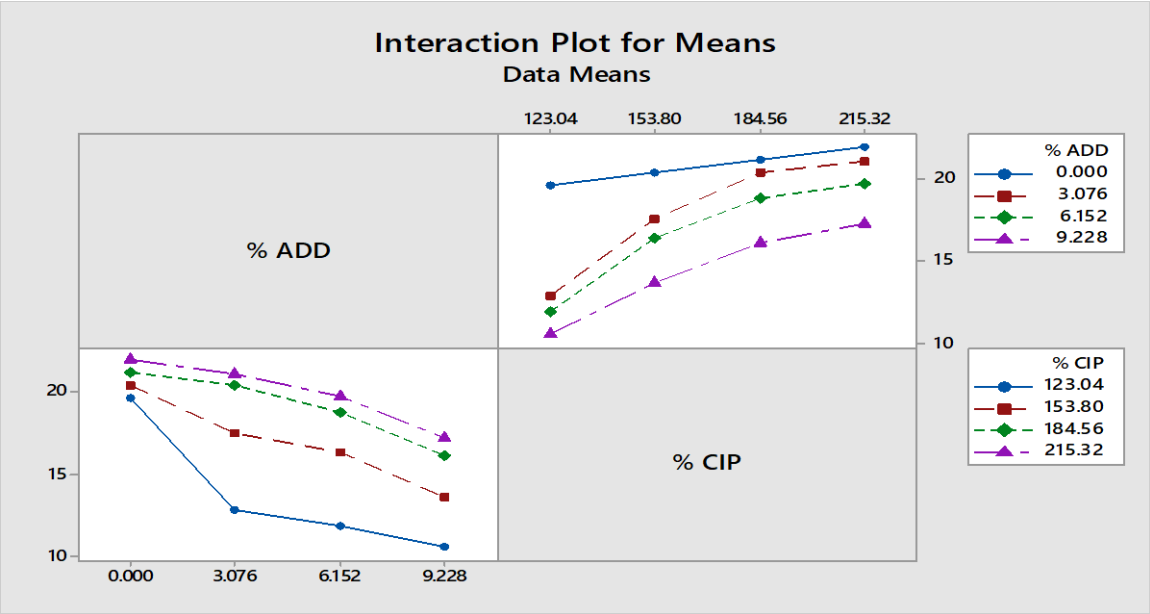

Figure 2: Interactions plot for Means

The effects of the additives and the CIP on the standard deviation of the responses are plotted in Figure 3. The curve for additive and CIP are not straight, thus having different slopes of different points of the lines for both additive and CIP. The slope value is highest for the line connecting points 0.000 and 3.076 of additive and least for the line connecting the points 3,076 and 6.152. For the CIP curve, the slope is highest for the line connecting the first and second points, and least for the line connecting the 3rd and 4th points. Overall, both additive and CIP affect the standard deviations, having slopes that are not horizontal.

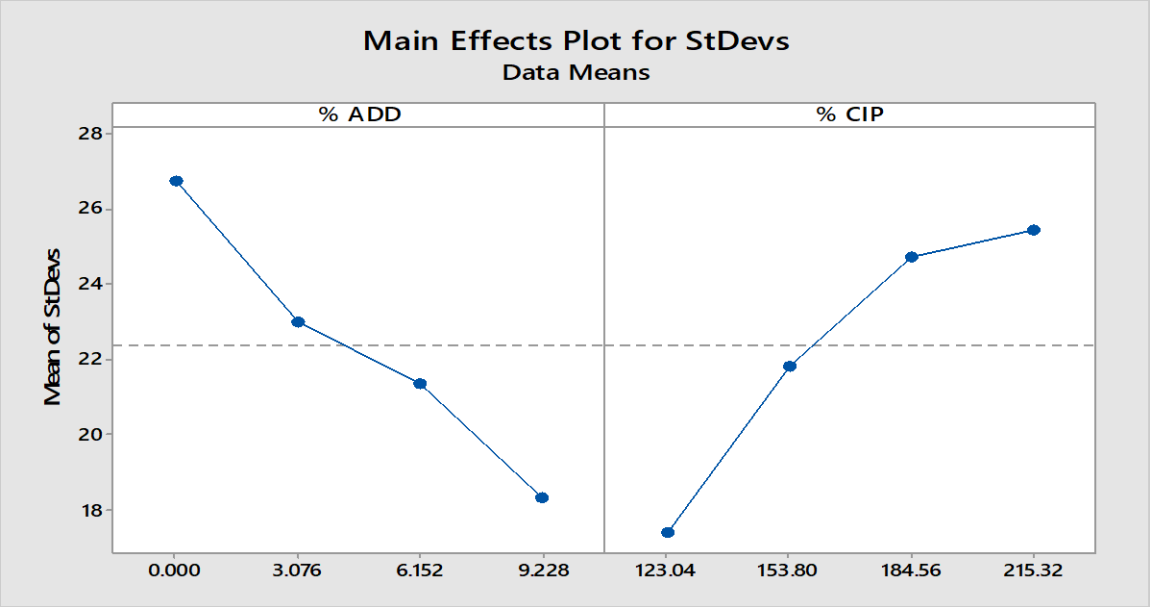

Figure 3: The main effect plots for standard deviations

In these plots shown in Figure 4, the interactions of the various factors regarding the standard deviations are presented. As observed, the first level of the additive has higher values, while the first levels of CIP have the highest sets of means. The fourth and fifth levels of additive are both parallel, while the second, third and fourth levels of CIP are parallel.

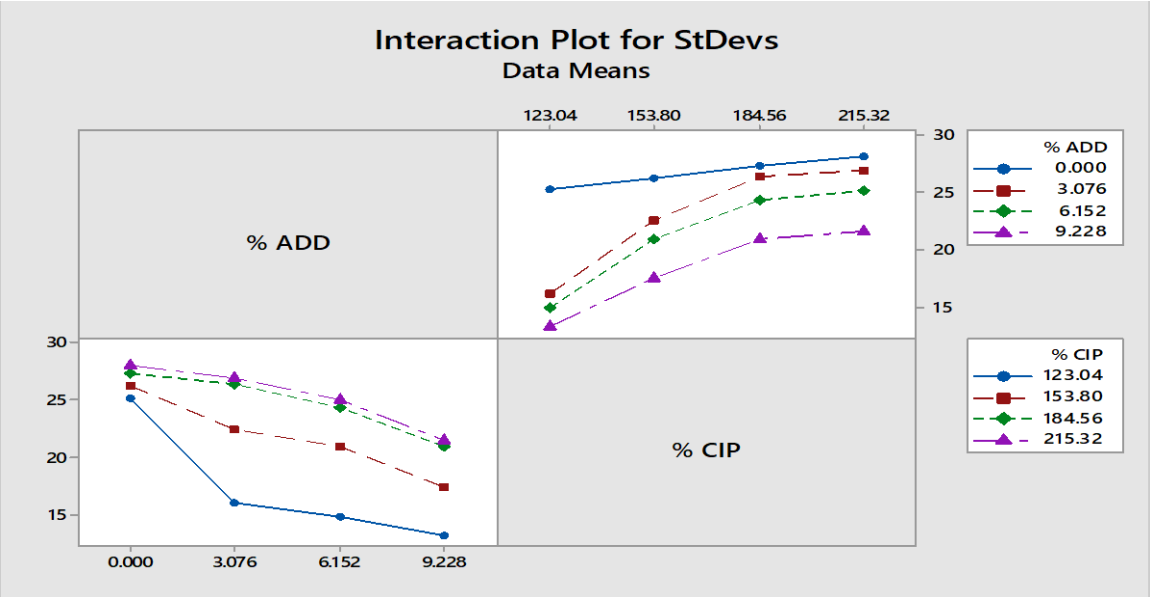

Figure 4: Interactions plot for the Standard deviation

The main effects plot of Signal-Noise ratio is given in Figure 5. Its shows that CIP has higher slope values within two corresponding points on its curve. The largest effect on the signal-to-noise ratio. On average, experimental runs with CIP had much higher signal-to-noise ratios than experimental runs with additives, having higher values of slopes for all points, while the additives had lines which are a bit more horizontal.

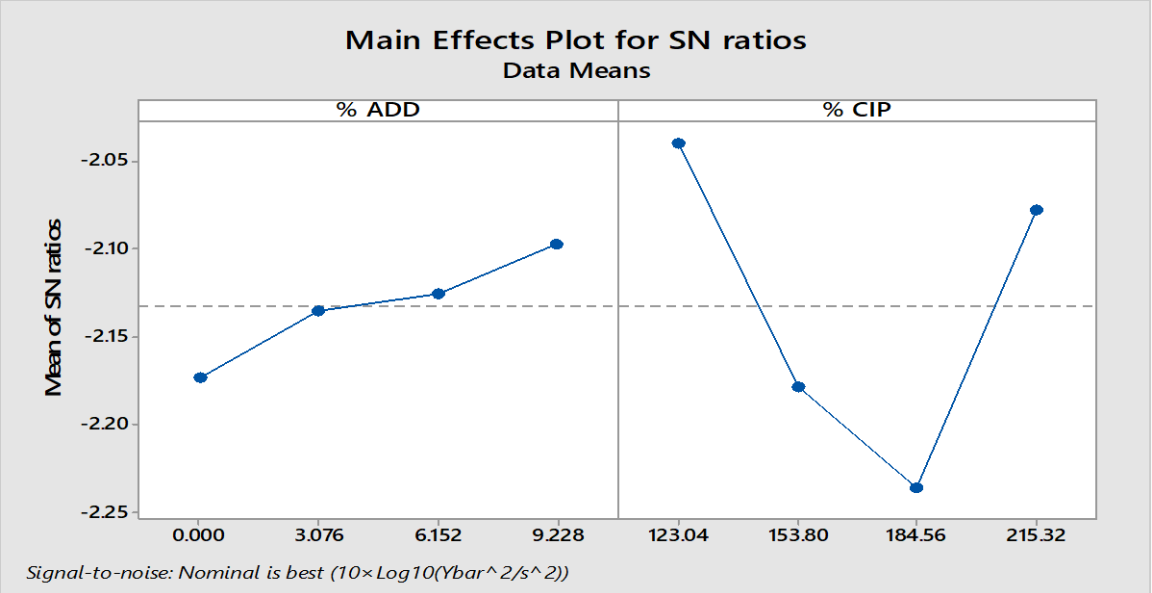

Figure 5: The main effect plot for SN ratios,

It is clear from the plot of the interactions of all input parameters on the signal-noise ratio shown in Figure 6 that the graphs are not parallel. This is an indication that there is an interaction between them. The fourth level of CIP has a higher SN ratio than additives.

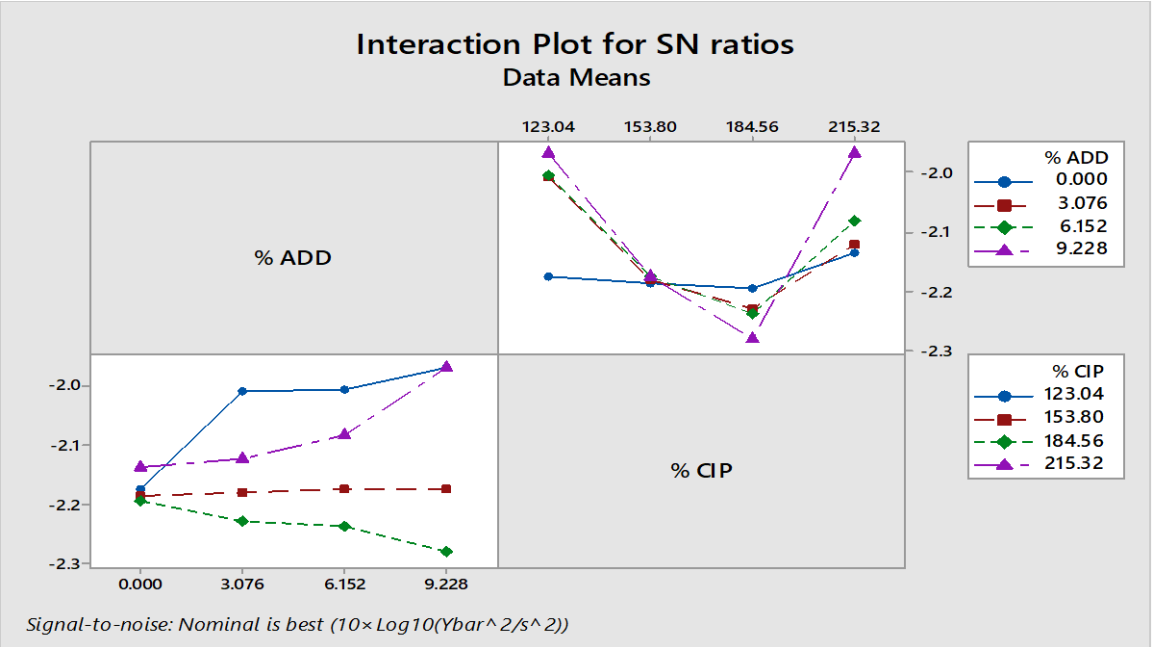

Figure 6: Interaction plot for Signal-Noise ratio

3.2 Results on RSM Box-Behnken Design

The design had 3 factors, 3 center points, 1 replicate, and 1 base block. The factors used for the analysis were the percentage by weight of the magnetic iron particles (CIP), additive (grease) and the percentage weight of base fluid (paraffin oil), and a total runs of 15 since it has just 1 replicate of the base number of runs. The design has a just 1 base block and 1 total block. The statistical details of the RSM model is presented in Table 4. The standard deviation (S) in kg is 0.035 which

is lower than all values of the factors used. The R-sq value of 99.37% explains that proportion in the set data, and since it is about 100%, the model perfectly fits the data. Another important figure from the table is the R-sq (pred.), which informs how well the model may predict new values of responses. The R-sq (pred.) which is 89.92% is sufficiently high being close to 100%, which is not different from the R-sq value and this conformed that the model does not over-fit the data set. The model equation is given in Equation 3.

Table 4: Model summary for sedimentation ratio

S	R-sq	R-sq(adj)	R-sq(pred)
0.0353553	99.37%	98.24%	89.92%

$$\boldsymbol{Sedimentation\ ratio = -122 + 250 * W_p - 0.056W_A - 0.43 * W_C - 125 * W_P^2 + 0.000611 * W_A^2 + 0.01667 * W_C^2 + 0.00444 * W_A * W_C} \quad (3)$$

Table 55 summarizes the variables used to ascertain the efficiencies of the model. As observed, the model adequately captures the responses of the input variables having R-sq value of 94.67, but would perform poorly when used to predict data outside the experiment data since the R-sq predicted value is 14.77 % being too low. The developed model is given in Equation 4.

Table 5: Model Summary for viscosity

S	R-sq	R-sq(adj)	R-sq(pred)
0.353553	99.37%	98.24%	89.92%

$$Viscosity = -18846 + 37750 * W_p + 0.11W_A - 8.9W_C - 1.8875W_p^2 + 0.0015W_A^2 + 0.372W_C^2 + 0.0633W_AW_c \quad (4)$$

The standardized sedimentation ratios were relative to the distribution fit line for cases where other effects are 0. The points are closely related to the line of fit, indicating that the model properly fits the experimental data. Additionally, the data was well distributed, as there is an equal number of samples on both sides of the normal (0 point).

Table 6 summarizes the variables used to ascertain the efficiencies of the model. As observed, the model adequately captures the responses from the input variables having R-sq value of 100% and would perform excellently when used to predict data outside the experiment data since the R-sq predict is 100.00 %. The developed model is given in Equation 5.

Table 6: Model Summary for yield stress

S	R-sq	R-sq(adj)	R-sq(pred)
5E-07	100%	100%	100%

$$Yiels\ stress = 0.0005 - 0.00005W_P - 0.000008W_A + 0.001106W_C + 0.00003W_P^2 + 0.000001W_A^2 - 0.000000W_C^2 - 0.000003W_A.W_C \quad (5)$$

The residual plots of the sedimentation ratio is shown in Figure 7. It can further be observed from plot of residual versus fitness values are higher than the confidence level (0.05) for all values of sedimentation ratio. Also, as shown by the histogram of residuals of the sedimentation model, it was observed that, for a data spread of -0.04-0.04, the residuals mode falls between -0.2 and 0.2, as the three bars have equal peak values greater than 2.5. Considering that the histogram can quickly form a normal curve, there are few outliers which constitutes a negligible proportion of the data set, but the fall within an acceptable value for residual being lesser than 0.5. The order plot of sedimentation ratio, which does not form any pattern, reveals the lack of correlation between the residuals, confirming that the data were not simulated, but rather contains an acceptable level of experimental errors. Lastly, the points on the normal probability plot of 15 are normalized values. The residual points are very close to the line of fit, and there are no points that are far off from the line of fit. This shows that the residuals value perfectly follows a normal probability curve.

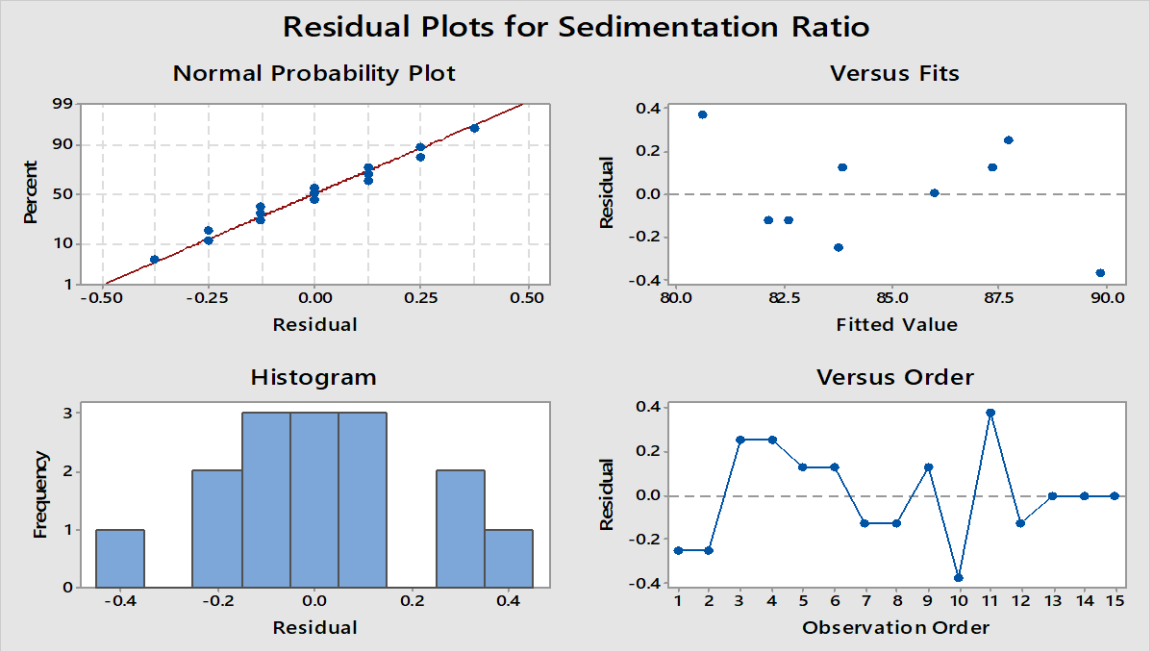

Figure 7: Residual plots for Sedimentation Ratio

A random pattern was observed for the fitted values versus their residuals, as seen in the residual versus fit plot in Figure 8, which confirms values of the factors (Additive, CIP and Paraffin) are not related to the residual values. Thus the model was a good replica of the experimental data. Additionally, as shown in the residual histogram for the viscosity response curve generated with RSM, a good proportion of the fitted data set has residual values between 0 and 0.05. However, there are a number of dataset with residual values higher than 0.05. The spread on the histogram forms a normal curve. The order of observations versus their residuals is presented as obtained from fitting the data set with the model. There is no correlation between the order and the residual dataset.

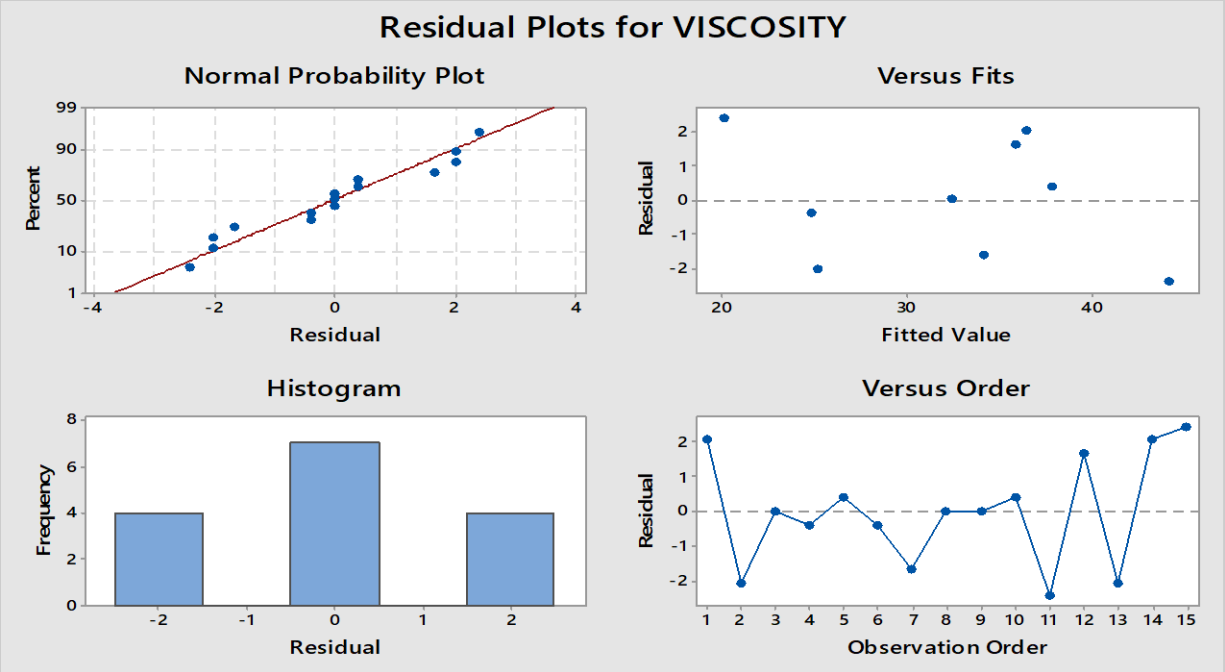

Figure 8: Residual Plots for Viscosity

The residual plots for yield strength are shown in Figure 9. Random patterns were observed for the fitted values versus their residuals, as shown in the residual versus fit plot in Figure 9, which confirms values of the factors (Additive, CIP and Paraffin) are not related to the residual values of yield stress. Thus the model was a good replica of the experimental data. Additionally, as shown in the residual histogram for the viscosity response curve generated with RSM, a good proportion of the fitted data set has residual values between 0 and 0.05. However, there are a number of dataset with residual values higher than 0.05. The spread on the histogram forms a perfect normal curve. The order of observations versus their residuals is also presented as obtained from fitting the dataset with a model. There is no correlation between the order and the residual values.

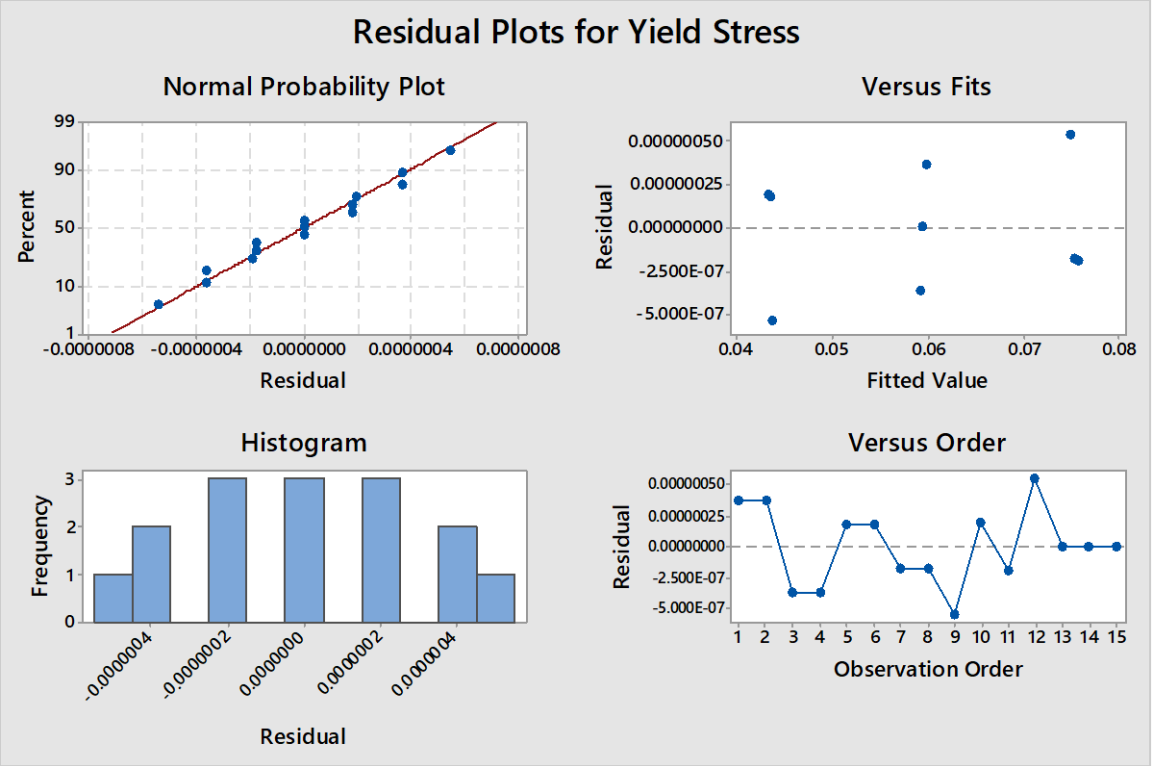

Figure 9: Residual plots for yield strength

The surface plots for the effects of combined factors on the Yield stress, sedimentation ratio and viscosity are shown in Figure 10 - 15. The percentage change in paraffin had minimal effects on the yield strength, as it was not largely varied since it is also a function of the proportion of other effects. It can be observed also that the yield stress increases with CIP, but decreases slightly with additive, whereas the effect of percentage volume had the least effect on the yield strength of the MRF. The values of yield stress increases directly with percentage by mass of CIP. This is in line with previous studies in which values of yield stress were found to increase with the proportion of added CIP [16], [17]. There is a slight decrease in yield stress with the value of additive added, but this is not very significant, as only a small proportion of additive is added for all samples. Maximum values of yield stress, however, is about 0.22 Pa, while the minimum value is about 0.13 Pa. This value compares favorably with commercially available MRF [18].

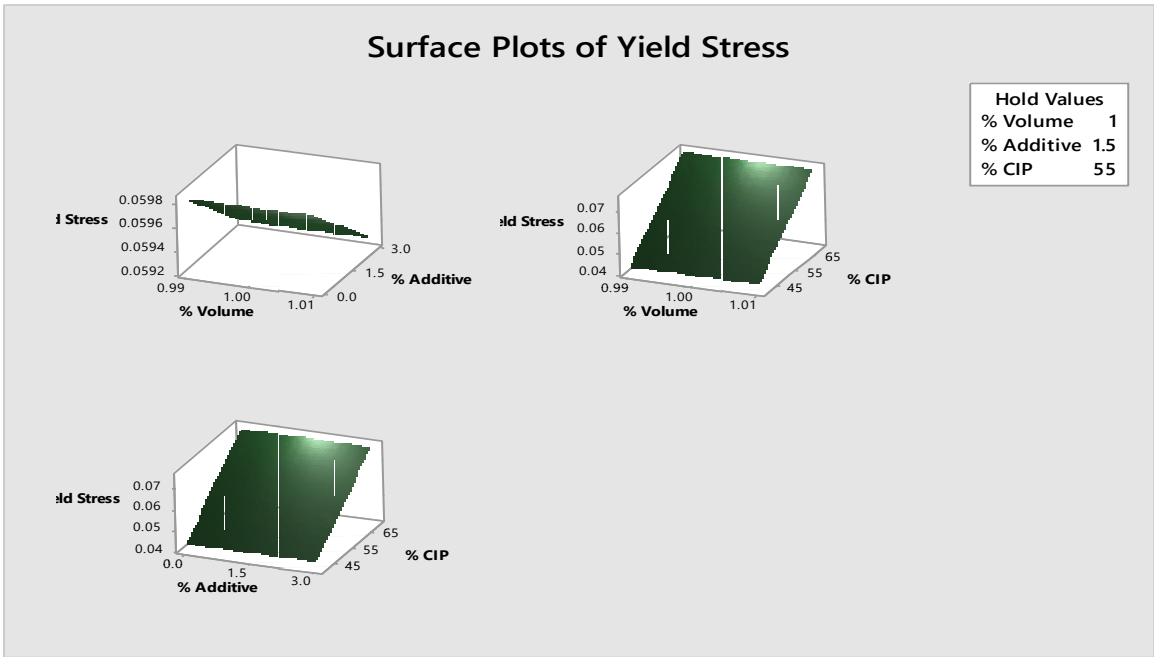

Figure 10: Surface plots of yield stress

As can be seen in Figure 11, sedimentation ratio, however, increases with the additive and decreases with the percentage CIP that was used in preparing the MRF while the volume had a negligible effect. This implies that proportion of CIP that would settled when the MRF is left for some time would increase with increasing proportion of CIP, and this is so because once the saturation point is reached, every other mass of CIP is expected to settle [19]. Additives are reportedly known to improve sedimentation properties as reviewed in the literature [9], [20], [21]. Stearic acid, which was used as an enhancer in this work, has been used in the past to improve sedimentation properties of MRF [7], [22], [23]. It was thus expected that higher proportion of CIP would remain suspended in the developed MRF when stearic acid is added as an additive.

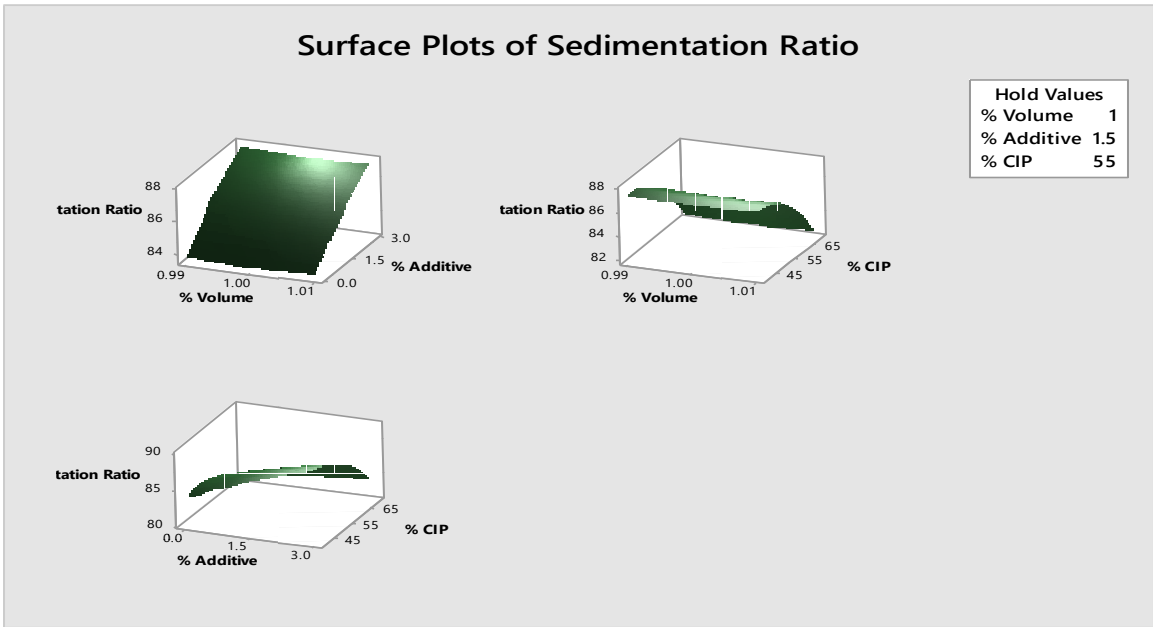

Figure 11: Surface plots for Sedimentation ratio

For viscosity, all effect had positive correlation with its values, as it can be seen that viscosity increased positively with both the additive, CIP and paraffin oil. Grease and CIP are denser than paraffin oil, so when mixed with the paraffin oil is expected to have increased values of viscosity since the added particles would offer resistance to flow. Additives generally are known to make carrier fluid more viscous, as this is the means by which sedimentation of magnetic particles is reduced. Previous studies have also reported the increasing values of viscosity with CIP [24], as well as stearic acid [7], [23].

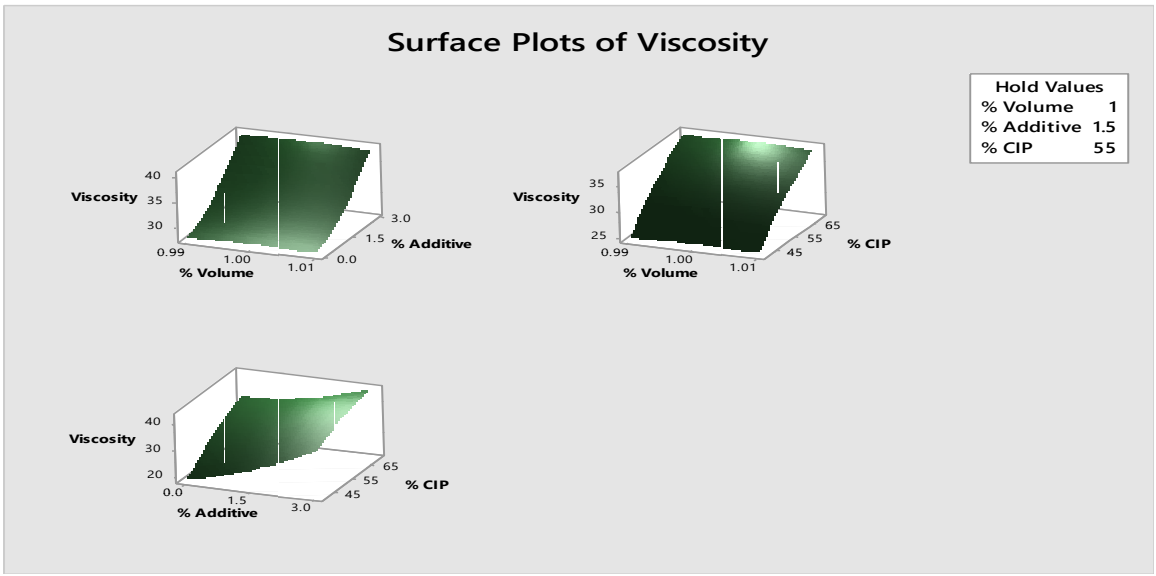

Figure 12: Surface plots for Viscosity

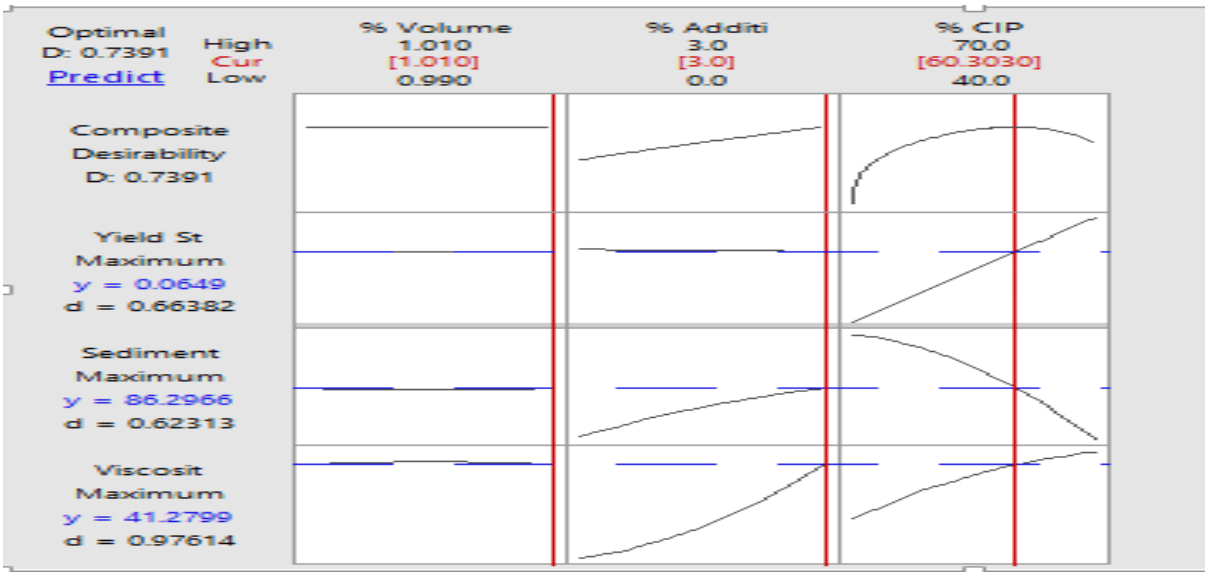

Figure 13: Optimization plot for the developed MRF

4.8 Optimization

The optimization plot is shown in Figure 13. It shows the optimal solutions of the plot. The input variables are shown in the columns, while the responses are the rows. The optimal CIP, Additive and Paraffin oil values were 60 %, 3% and 100%, respectively. The predicted values for yield stress, sedimentation ratio and viscosity are 0.66382, 86.2966 and 41.2799.

5.0 Conclusion

The high cost of silicone-based MRF, which is well researched and commercially available, has reduced their applicability in engineering. Thus, this work aims to develop and characterize a novel MRF suitable for flow-mode applications from cheap and readily available constituting materials. In pursuing the development of the new type of MRF, Carbonyl-iron particles (CIP), low viscosity paraffin oil, and Lithium grease were used as magnetic particle, base fluid, and additives, respectively. The concept of numerical optimization using both RSM and Taguchi method was employed to obtain the optimal combination of input parameters for optimum performance. So overall, a novel MRF from a combination of Paraffin oil, CIP and grease as enhancer having sufficient yield and stability was developed. The performance characteristics and optimum values were obtained using RSM and Taguchi Design of Experiment techniques. It was found that the optimal input parameters were 60% and 3% by weight of CIP and Lithium grease, respectively. The MRF was found to perform satisfactorily compared with other emerging MRFs, and it is suitably used for flow-mode applications.

References

[1] S. Bahl, H. Nagar, I. Singh, and S. Sehgal, "Smart materials types , properties and applications : A review," *Mater. Today Proc.*, 2020.
[2] H. Shokrollahi, "A review of the magnetic properties , synthesis methods and applications of maghemite," *J. Magn. Magn. Mater.*, vol. 426, no. July 2016, pp. 74–81, 2017.
[3] J. S. Kumar, P. S. Paul, G. Raghunathan, and D. G. Alex, "A review of challenges and solutions in the preparation and use of magnetorheological fluids," *Int. J. Mech. Mater. Eng.*, vol. 14, no. 13, pp. 1–18, 2019.
[4] R. Ahamed and S. Choi, "A state of art on magneto-rheological materials and their potential applications," vol. 29, no. 10, pp. 2051–2095, 2018.
[5] A. Hajalilou and E. Al, "Field Responsive Fluids as Smart Materials," *Eng. Mater.*, 2016.
[6] J. Oh and S. Choi, "A Review on the Development of Dampers Utilizing Smart Magnetorheo- logical Fluids," vol. 4658, no. 1, pp. 15–21, 2019.
[7] Y. Rabbani, M. Ashtiani, and S. H. Hashemabadi, "An experimental study on the effects of temperature and magnetic field strength on the magnetorheological fluid stability and MR effect," *R. Soc. Chem. Soft Matter*, pp. 1–8, 2015.
[8] I. Bica, Y. Dan, and H. Jin, "Physical characteristics of magnetorheological suspensions and their applications," *J. Ind. Eng. Chem.*, vol. 19, no. 2, pp. 394–406, 2013.
[9] B. Gopinath *et al.*, "A systematic study of the impact of additives on structural and mechanical properties of Magnetorheological fluids," in *Materials Today: Proceedings*, 2020, pp. 1–8.
[10] I. Bica, E. M. Anitas, L. Marina, E. Averis, S. Hyuk, and H. Jin, "Journal of Industrial and Engineering Chemistry Magnetostrictive and viscoelastic characteristics of polyurethane-based magnetorheological elastomer," *J. Ind. Eng. Chem.*, vol. 73, pp. 128–133, 2019.
[11] G. Wang, Y. Ma, Y. Tong, and X. Dong, "Journal of Industrial and Engineering Chemistry Development of manganese ferrite / graphene oxide nanocomposites for magnetorheological fl uid with enhanced sedimentation stability," *J. Ind. Eng. Chem.*, no. 2016, pp. 1–9, 2017.
[12] B. D. Chin, J. H. Park, M. H. Kwon, and O. O. Park, "Rheological properties and dispersion stability of magnetorheological (MR) suspensions," *Rheol. Acta*, vol. 40, pp. 211–219, 2001.
[13] M. A. Portillo and G. R. Iglesias, "Magnetic Nanoparticles as a Redispersing Additive in Magnetorheological Fluid," *J. Nanomater.*, vol. 2017, pp. 1–8, 2017.
[14] A. Kaide, M. Kanda, H. Tochigi, and T. Saeki, "Preparation of Magnetorheological Fluid Using Stabilizing Additives," vol. 02005, pp. 2019–2022, 2021.
[15] F. R. Cunha, A. P. Rosa, and N. J. Dias, "Rheology of a Very Dilute Magnetic Suspension with Micro-Structures of Nanoparticles," *J. Magn. Magn. Mater.*, pp. 1–27, 2015.
[16] D. Kittipoomwong, D. J. Klingenberg, and J. C. Ulicny, "Dynamic yield stress enhancement in bidisperse magnetorheological fluids," vol. 1521, no. May 2014, 2013.
[17] F. Vereda, J. de Vicente, J. P. Segovia-Guti´errez, and R. H.-A. Biocolloid, "Average particle magnetization as an experimental scaling parameter for the yield stress of dilute magnetorheological," *J. Phys. D. Appl. Phys.*, vol. 44, no. 425002, pp. 1–6, 2011.
[18] M. Nejatpour, U. Unal, and H. Y. Acar, "Bidisperse magneto-rheological fl uids consisting of functional SPIONs added to commercial MRF," *J. Eng. Chem.*, vol. 91, pp. 110–120, 2020.
[19] Y. Wang, W. Xie, and D. Wu, "Rheological properties of magnetorheological suspensions stabilized with nanocelluloses," *Carbohydr. Polym.*, vol. 231, no. September 2019, p. 115776, 2020.
[20] V. Kumar and D. Lee, "Journal of Magnetism and Magnetic Materials Mechanical properties and magnetic e ff ect of new magneto-rheological elastomers fi lled with multi-wall carbon nanotubes and iron particles," *J. Magn. Magn. Mater.*, vol. 482, no. March, pp. 329–335, 2019.
[21] M. Kumar, D. Dinakar, I. Mohan, and S. Jha, "Optik Experimental investigation and machine parameter optimization for nano finishing of fused silica using magnetorheological finishing process," *Optik (Stuttg).*, vol. 226, no. P1, p. 165908, 2021.
[22] G. Shi, W. Wang, G. Wang, F. Yang, and X. Rui, "Dynamic mechanical properties of FeSi alloy particles-filled magnetorheological elastomers elastomers," *Polym. Technol. Mater.*, vol. 00, no. 00, pp. 1–13, 2019.
[23] R. Asiaban, H. Khajehsaeid, E. Ghobadi, and M. Jabbari, "New magneto-rheological fluids with high stability : Experimental study and constitutive modelling," *Polym. Test.*, vol. 87, no. March, p. 106512, 2020.
[24] N. P. Sherje and S. V Deshmukh, "Synthesis and Optimization of Magneto-Rheological Fluid for Dampers of Suspension System," in *International conference on "Recent Advances in Interdisciplinary Trends in Engineering & Applications*, 2019.